ELSEVIER

Polymer 40 (1999) 5401–5406

polymer

The mass transport in poly(ethylene terephthalate) and related induced-crystallization

Hao Ouyang*, Shyh-Horng Shore

National Chung Hsing University, Institute of Materials Engineering, 250, Kuo Kuang Rd., Taichung 402, Taiwan, ROC

Received 10 July 1998; received in revised form 18 August 1998; accepted 27 October 1998

Abstract

The solvent transport in poly(ethylene terephthalate) (PET) and related phenomena were investigated. Based on Harmon's model for Case I (Fickian), Case II (swelling) and anomalous transport, the data of mass uptake were analyzed. Pure Case I or Case II behavior did not appear in our study and is affected by the annealing atmospheres and the preheating environments. The mass transport in PET is accompanied by a large-scale structural rearrangement, which leads to the induced crystallization of the original amorphous state. During this process, the matrix is under compressive stress. Solvent-induced crystallization was confirmed by X-ray diffraction (XRD), Differential Scanning Calorimeter (DSC), which is quite different from the thermal crystallization. The different behaviors of sorption between the solvent-treated PET crystallites and thermally treated PET can be explained in terms of the results of XRD, DSC and density measurement. © 1999 Elsevier Science Ltd. All rights reserved.

Keywords: Mass transport; PET; Induced-crystallization

1. Introduction

The transport of organic solvents in glassy polymer was discussed in terms of Fickian and swelling mechanisms [1]. The penetrant moves from the area with high concentration to that with low concentration. If swelling occurs, there are significant stresses built up in the matrix. Experimental results indicated that in certain cases both the mechanisms operate simultaneously. Alfrey et al. [1] mentioned that swelling is not important and transport is pure Fickian diffusion (or Case I) when penetrant concentration is low. At higher concentration, swelling to relieve internal stress becomes significant. Therefore, the transport is pure Case II, in which a sharp penetrating front is observed and moves at constant velocity. When Case I (or II) dominates, the amount of penetrant is proportional to $t^{1/2}$ (or t). However, when both mechanisms are important, the exponent of time is between 1/2 and 1 (or t). Kwei et al. [2–5] proposed a transport model to describe Cases I and II transport phenomena. Chau and Li [6] studied the transport of methanol in PMMA shear bands, in which Case I dominates. They also found that underformed PMMA behaved Case II. Harmon et al. [7,8] investigated the transport of methanol in deformed, crosslinked PMMA disks using a modified Kwei's equation. The preliminary effort was quite successful. However, the transport of organic solvents in semi-crystalline polymer has not been studied extensively by this modified equation. It prompted us to investigate the mass transport in a glassy amorphous PET. Amorphous PET can transform to semi-crystalline state by thermal annealing [9,10] and solvent treatment [11,12]. In this work, the absorption behaviors of acetone in PET under different preheating media are studied by this model. The transport phenomena of acetone in PET under oven preheating have been reported elsewhere [13,14]. Further studies like premelting are presented here. The structural changes occurring as a result of the solvent sorption and thermal annealing were examined by XRD, DSC and density measurement.

2. Experimental

The present work involves experimental studies of solvent absorption, XRD, DSC and mass density. The PET (PET12270) sheet was obtained from the Eastman Chemical Company, Kingsport, TN. The molecular weight of PET was measured by gel permeation chromatography (GPC) as $M_w = 34900$, $M_n = 12000$ and $M_z = 55000$. The initial stages of specimen preparation are similar for studies of the properties mentioned above. All specimens, excepting for the microstructural observation and DSC,

* Corresponding author.
E-mail address: houyang@dragon.nchu.edu.tw (H. Ouyang)

0032-3861/99/$ - see front matter © 1999 Elsevier Science Ltd. All rights reserved.
PII: S0032-3861(98)00764-2

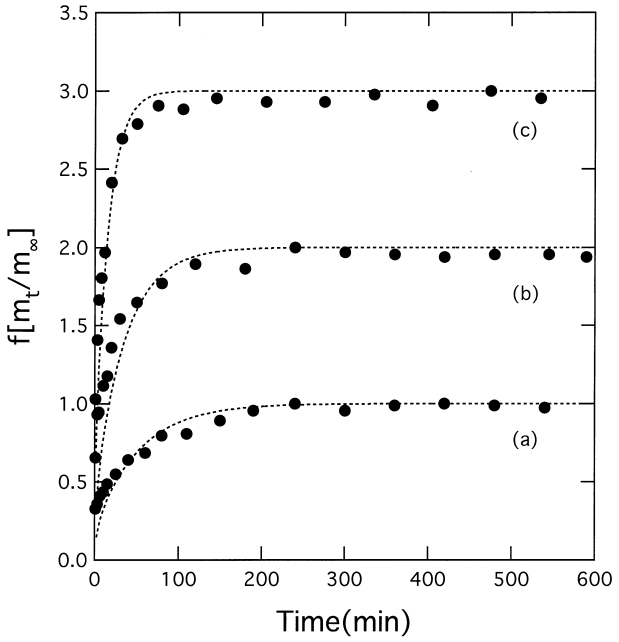

Fig. 1. Acetone absorption in PET as annealed in air then preheated in water (a) 30°C, $f = 1$, (b) 40°C, $f = 2$ (c) 50°C, $f = 3$.

were initially prepared as follows. Specimens of $10 \times 3.5 \times 0.5$mm were cut from the sheet and polished using 800-, 1200-, 1500- and 4000-grid carbimet papers, followed by final polishing with 1-, 0.5- and 0.05-μm alumina slurries. Specimens of $20 \times 20 \times 1$ mm for the X-ray diffraction measurement and of $3.5 \times 2 \times 0.5$ mm for the DSC study were prepared in a similar way. All the specimens were annealed in air or vacuum of 10^{-3} torr for 4 h at 70°C and

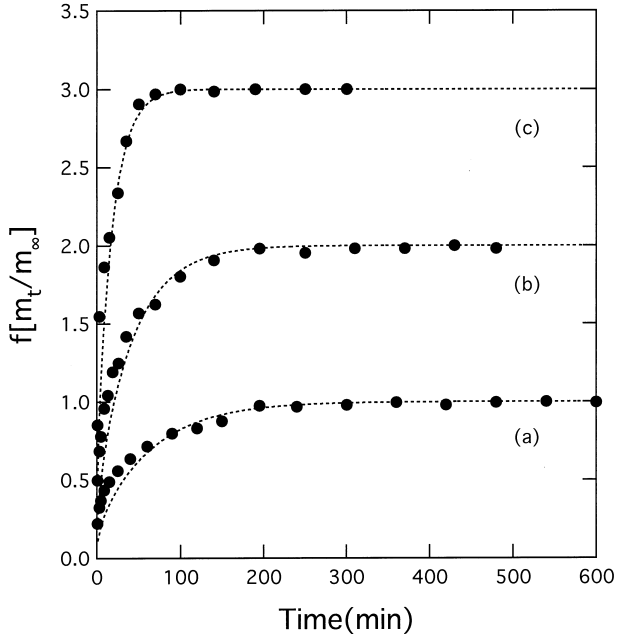

Fig. 2. Acetone absorption in PET as annealed in vacuum then preheated in water (a) 30°C, $f = 1$ (b) 40°C, $f = 2$ (c) 50°C, $f = 3$.

Table 1
The diffusivity D, velocity v and equilibrium solubility (ϕ) of mass transport for the samples preheated in the pure water

T(°C)	30	40	50
As annealed in the air:			
$D \times 10^8$ (cm^2/s)	3.0	6.0	10
$v \times 10^7$ (cm/s)	1.8	3.0	5.0
ϕ(g/g)	0.115	0.110	0.103
As annealed in vacuum:			
$D \times 10^8$ (cm^2/s)	2.4	3.7	8.5
$v \times 10^7$ (cm/s)	1.5	3.0	4.0
ϕ(g/g)	0.117	0.112	0.103

then furnace cooled to the ambient temperature, approximately 25°C. This process was performed in a EYELA VOS-200SD vaccum dry oven. In order to obtain the thermal crystallites, some specimens were annealed at 140°C for 4 h after 70°C heat treatment.

3. Absorption measurement

Each absorption sample was preheated in the oven or in the pure water for 15 min, then put in a glass test tube filled with acetone at the same temperature. This test tube is situated in a Neslab RTE-111 refrigerated bath/circulator in order to preserve constant temperature with an accuracy ±0.1°C. After a period of time, the sample was removed to measure its weight by a OHAUS AP250D digital balance. Then it was quickly returned to the test tube for the next interval of soak. The weight-gains versus time for the specimens annealed at 70°C then preheated in water are shown in Figs. 1 and 2. Here f is the scaling factor used to plot all the curves in one figure distinctly. However, for the PET annealed at 140°C, there is no change of weight observed within a week. The increase of weight versus time has been fitted according to Harmon's result [7] which accounts for Cases I, II, and mixed condition:

$$\frac{m_t}{m_\infty} = 1 - 2\sum_{n=1}^{\infty} \frac{\lambda_n^2(1 - 2\cos\lambda_n e^{-vl/2D})}{\beta_n^4(1 - (2D/vl)\cos^2\lambda_n)} e^{-\beta_n^2 Dt/l^2}, \quad (1)$$

where m_t/m_∞ is the absorbed mass of solvent at time t relative to the absorbed mass in saturation, l is the half-thickness of specimen, D and v are constant diffusivity and velocity respectively, and

$$\lambda_n = \frac{vl}{2D}\tan\lambda_n, \quad (2)$$

$$\beta_n^2 = \frac{V^2 l^2}{4D^2} + \lambda_n^2. \quad (3)$$

Harmon's model is based on the assumption that the specimen is initially solvent-free, and that solvent concentration is at all times constant on the surfaces of sample. By curve fitting from Figs. 1 and 2, the corresponding D and v listed in Table 1 can be obtained. The associated activation

Table 2
The activation energies of diffusivity D, velocity v and the enthalpies of mixing associated with the equilibrium solubility (ϕ) for the mass transport

	D	v	ϕ
As annealed in the air:			
(kcal/mol)	11.7	10.1	−0.466
As annealed in vacuum:			
(kcal/mol)	12.3	9.60	−0.533

energies listed in Table 2 can be calculated according to Arrhenius relationship as shown in Figs. 3 and 4. The equation of desorption was derived elsewhere [13].

4. DSC measurement

The specimens were obtained by cutting a rectangular parallelepiped of 3.5 × 2 × 0.5 mm from the solvent-saturated sample in the experiment of absorption. Relatively small sample thickness was used to minimize the effect of low thermal conductivity of the polymers. Each specimen with a mass of roughly l mg was placed in the receptacle of the Seiko DSC 6200 differential scanning calorimeter, equipped with a cooling accessory. The temperature and heat of melting were calibrated with inidium and tin. For the solvent-saturated specimen, the glass transition temperature decreases and the crystallization peak disappears [13,14]. In this work, the scanning rate is 15°C or 100°C min from 25°C to 300°C with a nitrogen flow of 40 ml/min. Both scanning rates show similar results. The DSC thermograms with 100°C/min are shown in Fig. 5. This highest scanning rate in this equipment was used to reduce the possibility of non-isothermal crystallization which might affect the premelting. The premelting temperatures are 110°C and 171°C for the PET samples desorbed at 40°C and annealed at 140°C respectively. The melting points

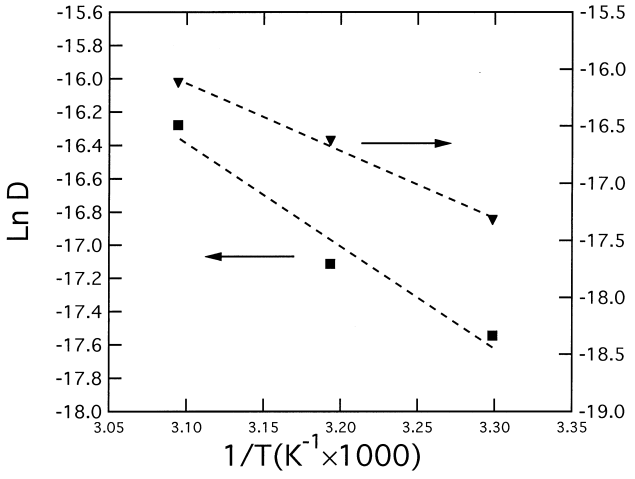

Fig. 3. Absorption Arrhenius plot of D in unit of cm^2/s, the data associated with left axis is for the sample annealed in vacuum, the other is for the samples annealed in air.

for both samples are around 250°C. The heat of fusion associated with 171°C is about 4.0 J/g. As the peak at 110°C is so broad to overlap another peak at 75°C which is the glass transition temperature of amorphous PET, it is hard to calculate the heat of this peak accurately. However, the area of peak at 171°C for the untreated PET can be estimated qualitatively larger than that at 100°C for the desorbed PET.

5. X-Ray measurement

The θ–2θ X-ray diffractometry was performed in a MAC MO3X-HF diffractometer using digital data acquisition and graphite-monochromated CuKα radiation detected by a scintillation counter. The operation conditions were set at 40 kV and 30 mA. The results of intensity versus 2θ are presented in Fig. 6. Before absorption experiment, the specimen annealed at 70°C still remained amorphous. It partly becomes crystalline after acetone absorption, desorption and annealing at 140°C.

6. Density measurement

The mass density measurement was performed with a OHAUS Density Determination Kit P/N 77402-00 in the OHAUS AP250D digital balance. It utilizes the Archimedes' principle [15]. The mass density is 1.389, 1.351, 1.355, 1.357, and 1.337 g cm^{-3} for the specimens annealed at 140°C, after absorption at 30°C, 40°C, 50°C and before absorption respectively. There is almost no difference in the density between the samples as prepared in the air and vaccum.

7. Results and discussion

The logarithms of solubilities listed in Table 1 versus reciprocals of temperatures are lotted in Fig. 7 and satisfy the van't Hoff plot of the specimens preheated in the pure water. The negative sign of the enthalpy of mixing listed in Table 2 as obtained from Fig. 7 means that the absorption process is exothermic. The solubilities of pure water at 30°C, 40°C, and 50°C for 15 min are negligible. The van't Hoff relationship can not be found as the sample was annealed in air then preheated in the oven [13,14]. And the Arrhenius plot of v for the samples prepared in air then preheated in the oven cannot be fitted quite well also by checking the chi-square of curve fitting [13,16] unless preheated in the pure water. Therefore, the mass transport of acetone in PET was affected by both annealing atmosphere [17,18] and preheating medium.

The mechanism of recrystallization-remelting [9,19–24] has been proposed for the interpretation of double melting peaks in PET. The recrystallization–remelting mechanism proposes that crystallization at lower temperatures can produce crystals with only a low degree of perfection or

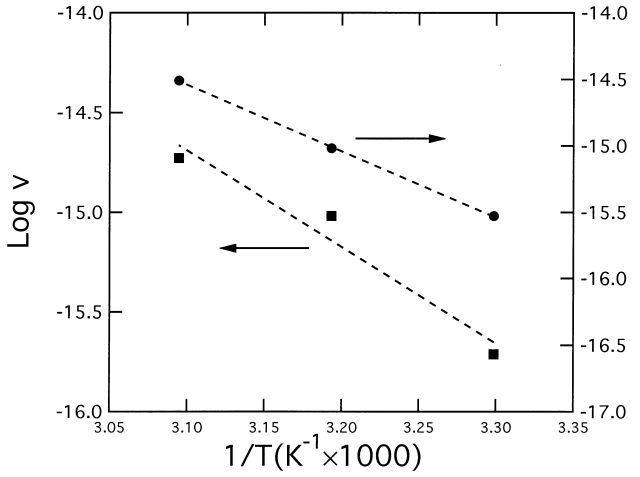

Fig. 4. Absorption Arrhenius plot of v in unit of cm/s. the data associated with left axis is for the sample annealed in vaccum, the other is for the samples annealed in air.

smaller size. The thickness of crystals can become larger after melting and re-crystallization. This process can occur upon a heating scan to a higher temperature during DSC thermal scanning [24]. A theoretical expression for the observed melting temperature, T_m, of a chain-folded polymer crystal is given by the Thomson–Gibbs equation [25]:

$$T_m = T_m^0\left(1 - \frac{2\sigma_e}{\Delta H^0 L}\right) \quad (4)$$

where T_m^0 is the melting temperature of an infinitely thick and perfect crystal, ΔH^0 is the heat of fusion, σ_e is the specific end-surface free energy of the crystals and L their thickness. The premelting temperature, 171°C, of the untreated PET annealed at 140°C is higher than that, 110°C, of the PET after absorption and desorption at 40°C. And the final melting points of the two samples are the same. These final endotherms corresponding to peak III [26–29] are attributed to fusion of crystals recrystallized and perfected during the DSC experiment itself. Peak II [29] is not obvious in this case since the sample was annealed below 160°C. The comparison of premelting temperatures implies that the average thickness of crystal for PET annealed at 140°C is larger than that of treated PET. However, the results obtained by this technique alone do not inform the exact morphology and there is a small endotherm about 170°C for the PET desorped at 40°C. Therefore, other analytical methods mentioned below are needed.

According to the X-ray diffraction data, no peak exists for the untreated PET annealed at 70°C which is the same as that of untreated PET without sample preparation. The structures of PET after absorption or desorption at 40°C and annealing at 140°C becomes semi-crystalline respectively. Similar results were obtained for treated PET at other temperatures [13,14]. The eight peaks of XRD pattern can be identified as $(0\bar{1}0)$, (010), $(\bar{1}11)$, $(\bar{1}10)$, (100), $(1\bar{1}1)$, $(0\bar{2}1)$ respectively [10]. The crystallinity of absorbed sample was not as strong as the specimen annealed 4 h at 140°C as indicated by the sharpness of diffraction peaks. Both structures are the same [30]. The broadening of the X-ray diffraction peaks can be attributed to the size and strain effects. After subtraction of amorphous part by using Fig. 6(a), these information can be obtained by the

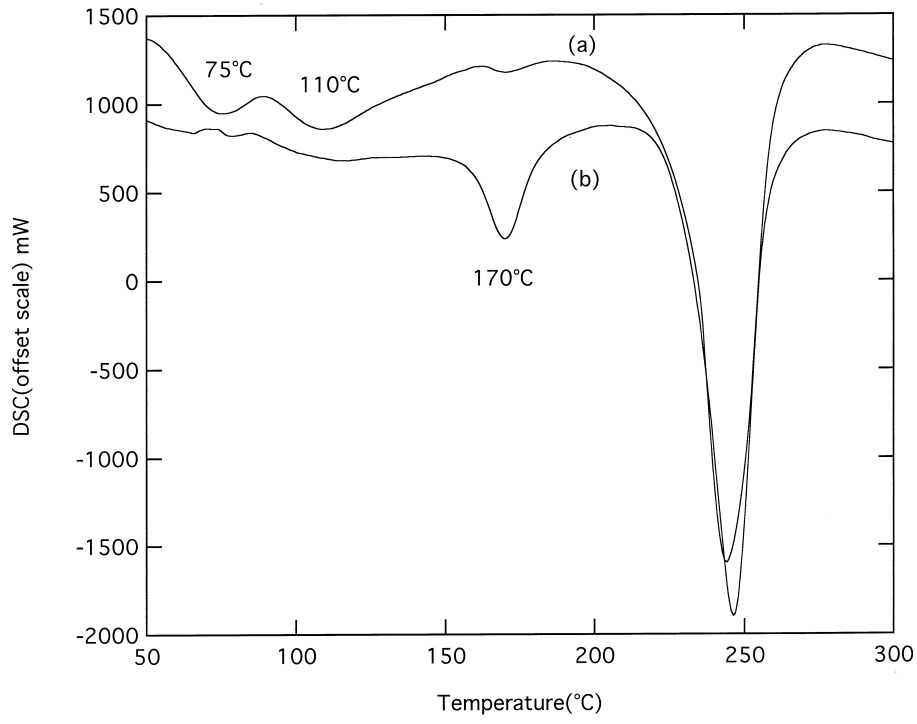

Fig. 5. DSC melting thermograms of PET (a) absorbed and desorbed at 40°C (b) annealed at 140°C.

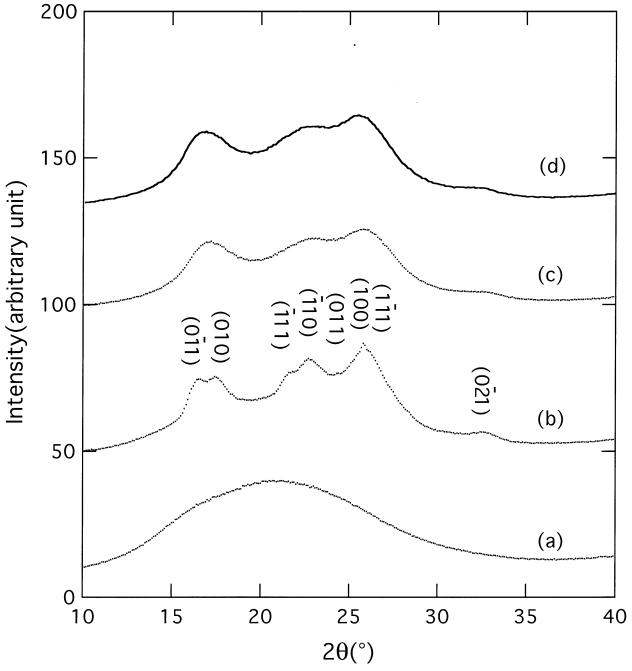

Fig. 6. X-ray patterns of (a) annealing at 70°C (b) annealing at 140°C (c) absorption at 40°C (d) desorption at 40°C.

Levenberg–Marquardt method, which optimizes the result of curve fitting for several peaks [16]. If the size and distortion line profiles are both presumed to be Cauchy [31], the grain size of PET treated at 40°C can be obtained as about 30 Å and the sample is under compressive stress from the plot of k (diffraction vector or the order of the diffraction) versus Δk (from the half-width-at-half-maximum of the linewidth) as shown in Fig. 8. Three data points in Fig. 8 correspond to Bragg angles at 11.5°, 13.3° and 16.4° respectively. The size can be obtained from the intercept of the curve fitting of the straight line in the plot and the negative

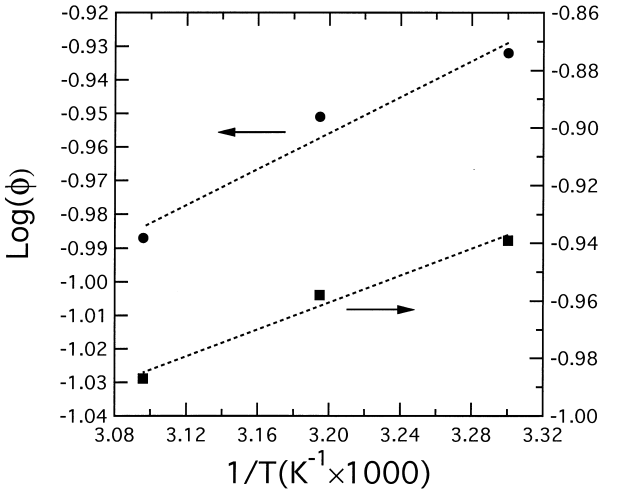

Fig. 7. Van't Hoff plot of solubility, the data associated with left axis is for the sample annealed in vacuum, the other is for the samples annealed in air.

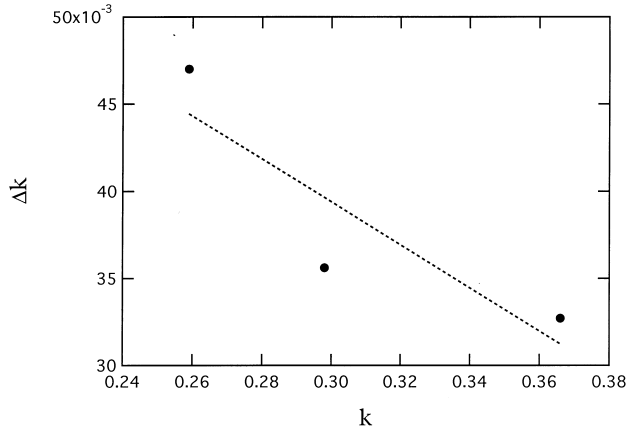

Fig. 8. Δk versus k of the acetone-treated sample.

slope indicates that the specimen is under compression. The compressive stress can be considered as an additional pressure in the imbibed liquid which affects the chemical potential [32]. This stress associated with volume expansion helps to pull out the loops of chains and makes the crystallization easier. The thickness of sample after saturated absorption usually increases about 10 percent, which also suggests that the specimen is under compressive condition. The size of PET annealed at 140°C is about two times larger, which is in the same order as obtained by small-angle X-ray diffraction [33].

The specific gravity is 1.389, 1.351, 1.355, 1.357, and 1.337 for the specimens annealed at 140°C, acetone-treated at 30°, 40°, 50°C, and before absorption respectively. The decreases in density are related to the decreased crystallinity, since the density of crystalline is much larger than that of amorphous phase [10,34]. If the densities of amorphous and crystalline phases are assumed to be constants, the weight fraction crystallinity, Wc, can be derived from [35]:

$$Wc(\rho) = [\rho_c(\rho - \rho_a)]/[\rho(\rho_c - \rho_a)] \quad (5)$$

where ρ represents the measured density, ρ_c and ρ_a are the densities of a perfect crystal and that of a completely amorphous specimen respectively. The widely accepted value of ρ_c is 1.455 g cm^{-3} [10] and ρ_a is 1.337 g cm^{-3} as measured in our experiment. The crystalline fractions of PET annealed at 140°C and after absorption are 0.46 and 0.12 respectively. The presence of perfect crystallites is the common cause of the absence of solubility [36]. This explains why the untreated PET annealed at 140°C is much more difficult for acetone to absorb than the PET annealed at 70°C.

8. Summary

Acetone transport in poly(ethylene terephthalate) and related phenomena have been investigated. Some important results are as follows:

1. The data of gravimetric sorption are analyzed by the sorption model proposed by Harmon et al. [7]. The

Case I diffusivity and Case II velocity for the best curve fitting satisfy the Arrhenius equation. Pure Case I or II behavior did not appear in this study.

2. The saturation acetone for the PET preheated in the pure water follows the van't Hoff plot. This relationship can not be observed if the specimen was annealed in the air then preheated in oven.
3. The specimen after 70°C annealing still remained amorphous. It was partly transformed into crystalline after acetone absorption, desorption and annealing at 140°C.
4. Both the XRD pattern and DSC curve show that the untreated PET annealed at 140°C and acetone-treated PET annealed at 70°C have crystallites. And the size of crystallites in the untreated PET annealed at 140°C is larger than that of treated PET.
5. The treated PET is under compressive stress. This stress can help the crystallization occur at lower temperatures.
6. The mass densities of the untreated PET and acetone-treated PET at 30, 40, 50°C and untreated at 140°C are 1.337, 1.351, 1.355, 1.357, and 1.389 g/cm^3, respectively. It shows that the thermally induced crystalline samples contain about 50% perfect crystallites and are much more dense than the solvent-induced crystallites. Therefore, the untreated PET annealed at 140°C is almost impervious to acetone uptake.

Acknowledgements

This work was supported by the National Science Council, Taiwan, Republic of China.

References

[1] Alfrey T, Gurnee EF, Lloyd WG. J Polym Sci (C) 1966;12:249.
[2] Wang TT, Kwei TK, Frish HL. J Polym Sci A-2 1969;7:2019.
[3] Kwei TK, Wang TT, Zupko HM. Maromolecules 1972;5(5):645.
[4] Kwei TK, Zupko HM. J Polym Sci A-2 1969;7:867.
[5] Wang TT, Kwei TK. Macromolecules 1973;6:919.
[6] Chau CC, Li JCM. Philos Mag 1981;A44:493.
[7] Harmon JP, Lee S, Li JCM. Polym Sci: Part A: Polymer Chemistry 1987;25:3215.
[8] Haromon JP, Lee S, Li JCM. Polymer 1988;29:1221.
[9] Fontaine F, Ledent J, Groeninckx G, Reyamaers H. Polymer 1982;23:185.
[10] Kitano Y, Kinoshita Y, Ashida T. Polymer 1995;36(10):1947.
[11] Makarewicz PJ, Wilkes GL. J Polym Sci Polym Phys Ed 1978;16:1529.
[12] Jameel H, Noether HD, Rebenfeld L. J Appl Polym Sci 1982;27:773.
[13] Hao Ouyang, Che-Chen Chen. J Appl Phys 1997;81(10):6680.
[14] Hao Ouyang, Che-Chen Chen, Sanboh Lee, Hsinjin Yang. J Polym Sci: Part B: Polymer Physics 1998;36:163.
[15] Halliday D, Resnick R. Fundamentals of physics. Singapore: John Wiley, 1981:274.
[16] Press WH, Teukolsky SA, Vetterling WT, Flannery BP. Numerical recipes in C. New York: Cambrige Univ. Press, 1992:620, 683.
[17] Holden PS, Orchard GAJ, Ward IM. J Polym Sci Polym Phys Ed 1985;23:2295.
[18] Orchard CAJ, Spiby P, Ward IM. J Polym Sci: Part B: Polymer Physics 1990;28:603.
[19] Holdsworth PJ, Turner-Jones A. Polymer 1991;12:195.
[20] Alfonso GC, Pedemonte E, Ponzetti L. Polymer 1979;20:104.
[21] Sweet GE, Bell JP. J Polym Sci A-2 1972;10:1273.
[22] Lin SB, Koenig JL. J Polym Sci Polym Phys Ed 1983;21:2365.
[23] Roberts RC. Polymer 1969;23:185.
[24] Woo EM, Ko TY. Colloid Polym Sci 1996;274:309.
[25] Hoffman JF. SPE Trans 1964;4(4):1.
[26] Lin S, Koenig JL. J Polym Sci Polym Symp 1984;71:121.
[27] Roberts RC. J Polym Sci Polym Lett 1970;8:381.
[28] Wunderlich B. Macromolecular physics crystal melting, 3. New York: Academic Press, 1980.
[29] Zhou C, Clough SB. Polym Eng Sci 1988;28(2):65.
[30] Sheldon RP, Plakey PR. Nature 1962;195:172.
[31] Klug HP, Alexander LE. X-ray diffraction procedures. New York: John Wiley, 1974:661.
[32] Silberberg A. Macromolecules 1980;13:742.
[33] Santa Cruz C, Stribeck N, Zachmann HG, Baltá Calleja FJ. Macromolecules 1991;24:5980.
[34] Fakirov S, Fischer EW, Schmidt GF. Makromol Chem 1975;176:2459.
[35] Alexander LE. X-ray diffraction methods in polymer science. New York: Wiley Interscience, 1969:189.
[36] Gedde UW. Polymer physics. London: Chapman & Hall, 1995:161.